M1 ICFP - Experimental physics
Cavity electrodynamics with ferromagnetic materials

Samuel Peyrière, Unai Trujols González

Abstract

When a microwave field shines on a ferromagnet under an external strong uniform magnetic field, the ferromagnet can absorb the microwave power if the wave's frequency is close to the Larmor frequency. This is the ferromagnetic resonance (FMR) effect. When the ferromagnet is placed inside a cavity, the FMR can be coupled to the electromagnetic modes of the cavity, leading to an avoided crossing. In this experimental project, we observe this phenomenon with YIG ferromagnets after characterizing all the elements of the setup individually. We provide a numerical simulation in good agreement with the experimental results and discuss the limits of our experiment.

Keywords— ferromagnetic resonance, avoided crossing, YIG ferromagnet, RedPitaya, QuTip

Introduction

Ferromagnetic resonance was first observed accidentally by V. K. Arkadiev in 1911. After the discovery of Larmor precession resonance for magnetic moments, enthusiasm built up around magnetic resonance phenomena in general (nuclear magnetic resonance, electron magnetic resonance, etc). Later independent observations of FMR by J. H. E. Griffiths [1] and E. K. Zavoiskij confirmed this phenomena but it wasn't until Kittle's 1945 seminal article [3] that a theory interpreted FMR experimental results successfully. An exhaustive study of FMR provides information on the magnetization, magnetic anisotropy, relaxation times, as well as the damping in the magnetization dynamics. Today, FMR is mainly used as a spectroscopic technique to probe small magnetic samples [4].

In this project, we will investigate this phenomena in a prototypical setup. A small ferromagnet is placed inside a microwave cavity. An external magnetic field generated by an electromagnet induces the precession of the spins. The sample interacts with incident microwaves and absorbs part of the field. It is key to interface properly the instruments in order to acquire transmission spectra and compare them to theoretical predictions.

1 Materials and theory

1.1 Ferromagnetic resonance (FMR)

Ferromagnetic resonance results from the coupling of an electromagnetic wave and the magnetization $\vec{M}$ of a ferromagnetic material. To describe it, we will follow Kittel's approach [2]. Consider a single crystal of a ferromagnetic material of magnetization $\vec{M}$ in an external magnetic field $\vec{H}$ with two contributions: a strong uniform and static field H_z and an incoming microwave field H_x of angular frequency ω propagating in the (Ox) direction. This field exerts a torque on the magnetization:

$$\frac{\partial \vec{M}}{\partial t} = \gamma \left(\vec{M} \times \vec{H} \right) \tag{1}$$

where γ is the gyromagnetic ratio. This causes the magnetization to precess around the DC field. Under the assumptions of a single ferromagnetic domain and neglecting the magnetic anisotropy forces, this set of differential equations is solved and the magnetic susceptibility $\chi_x = M_x/H_x$ is found to be:

$$\chi_x = \frac{\chi_0}{1 - (\omega/\omega_0)^2} \tag{2}$$

where χ_0 is the static susceptibility which depends on the biasing field and ω_0 is the Larmor angular frequency. This susceptibility becomes infinite at resonance when $\omega = \omega_0$. In practice, the microwave power is absorbed by the precessing magnetization and then lost as heat: this causes the resonance to have a finite value and a given width. The outgoing microwave field is strongly attenuated at resonance: we expect the power loss to be proportional to the susceptibility, and therefore to be a Lorentzian centered on ω_0 of a certain width. In his article, Kittel treats

this relaxation phenomena purely phenomenologically.

In a later article [3], Kittel extends the theoretical considerations mentioned previously. He justifies that the Larmor frequency ω_0 depends on the geometry of the crystal, its orientation and its shape. He provides a general formula generalizing the previously given $\omega_0 = \gamma \left(B_z H_z\right)^{1/2}$. He also mentions that a quantum mechanical treatment of the problem by Van Vleck leads to the same resonance conditions as his classical arguments.

1.2 FMR in a microwave cavity

Even if the classical picture of FMR provides precious insights into this phenomenon, a quantum approach is needed to understand its coupling to cavity modes. FMR is viewed as a spin wave in this approach, which can exchange excitations with an electromagnetic wave. If we consider a system formed by a single cavity mode and the atomic spins of the ferromagnet, this exchange phenomena is described in [5] by the Hamiltonian:

$$\hat{H}/\hbar = \omega_c \hat{a}^\dagger \hat{a} + g\mu_B B_z^{eff} \hat{S}_z + g_{FMR} \left(\hat{a}\hat{S}_+ + \hat{a}^\dagger \hat{S}_-\right) \tag{3}$$

where ω_c is the cavity mode angular frequency, $\hat{a}$ and $\hat{a}^\dagger$ the annihilation and creation operators for the mode, g the electron's g-factor and $\hat{\vec{S}}$ the collective spin operator for the ferromagnet. We write S the total spin norm. By re-writing the spin operator in terms of a Holstein-Primakoff boson in the limit of low-lying excitations:

$$\hat{S}_+ = \sqrt{2S}\hat{b}^\dagger \text{ and } \hat{S}_- = \sqrt{2S}\hat{b} \tag{4}$$

we can rewrite the Hamiltonian as:

$$\hat{H}/\hbar = \omega_c \hat{a}^\dagger \hat{a} + \omega_0 \hat{b}^\dagger \hat{b} + \tilde{g}\left(\hat{a}\hat{b}^\dagger + \hat{a}^\dagger \hat{b}\right) \tag{5}$$

The introduction of the bosonic operators $\hat{b}$ and $\hat{b}^\dagger$ allows us to introduce a quasi-particle, the magnon, associated to the spin waves. The eigenvalues of $\hat{b}^\dagger \hat{b}$ is the number of such magnons in the ferromagnet. The right term of the Hamiltonian accounts for the fact that a magnon can be destroyed if a photon in the mode is created and conversely, the ferromagnet can absorb a photon by creating a magnon. $\tilde{g}$ describes the strength of the cavity-magnon coupling. The states $|n_{phot}, n_{mag}\rangle$ are not eigenstates of $\hat{H}$. Therefore, when we vary B and consequently ω_0, the FMR and the cavity modes resonance cross one another. We expect to see an avoided crossing of the eigenenergies. This is the phenomenon that we ultimately want to observe in this project.

2 Setup and methods

2.1 Setup

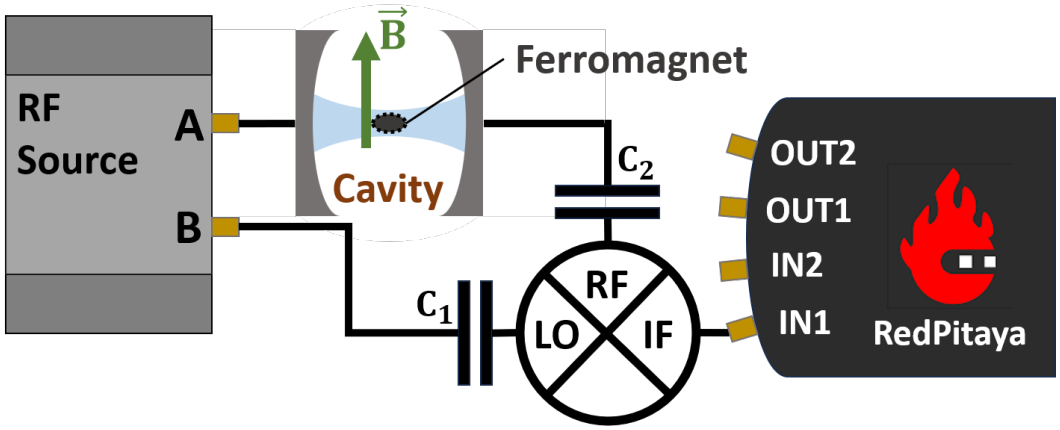

Figure 1: **Setup to acquire transmission spectra.** The RF source generates two microwave (MW) electronic signals, one going through the MW cavity and the other going directly to the mixer. $\Delta f = f_A - f_B$ is fixed to 10 MHz, while f_A varies from 2 GHz to 12 GHz. The capacitors C_1 and C_2 protect the mixer by filtering out an eventual constant voltage. The mixer down-converts the signal of interest coming into the RF port to obtain a 1 MHz signal. The RedPitaya acquires around a hundred periods, performs and analog/digital conversion. A computer then computes the standard deviation (std) of the sinusoidal signal, proportional to its amplitude. This amplitude is itself proportional to the transmission of the system {cavity + mixer} assuming that the source power is constant during an acquisition

The goal of this project is to observe the coupling of ferromagnetic resonances and cavity modes. We will first describe the setup used to observe this effect (Fig. 1). We will then provide details about the successive steps we took to correctly assemble the experiment.

We place a small YIG ferromagnet inside a rectangular microwave cavity (the exact placement of the ferromagnet in the cavity will be discussed later). YIG is actually a ferrimagnetic material. Such materials have populations of opposing spins as in antiferromagnets, but the magnetic moments are unequal in amplitude, giving rise in practice to a ferromagnetic material. The cavity is placed between the two plates of an electromagnet which generates a normal uniform magnetic field. We send microwaves through the cavity generated by the RF source (port A) which frequency f_A may vary in the range $2-12$ GHz. Source B generates a microwave signal of frequency $f_B = f_A - \Delta f$ where we have set $\Delta f = 10$ MHz. The output of the cavity and the reference signal are mixed in order to produce a signal of frequency $\Delta f = 10$ MHz which the RedPitaya can detect. The capacitors protect the mixer by filtering out an eventual DC component of the voltage.

We interface the RF source, the electromagnet and the RedPitaya with a computer in order to acquire the transmission of the microwaves depending on the externally imposed magnetic field and the microwave frequency. In the following parts, we will investigate in detail the effect of each component of the setup in order to finally understand the collective behaviour of the system under investigation.

2.2 Characterization of the cavity

We first estimated the theoretical selected modes for an empty microwave cavity, that we then compared to a transmission spectrum. We were given two rectangular copper cavities: a large one of dimensions $50 \times 35 \times 5$ mm and a small one of dimensions $50 \times 18 \times 5$ mm. If the cavities were perfectly conducting and without geometric defects, we would expect the eigenfrequencies of the cavity modes TE_{mnl} and TM_{mnl} to be given by:

$$f_{mnl} = \frac{c}{2}\sqrt{\left(\frac{m}{a}\right)^2 + \left(\frac{n}{b}\right)^2 + \left(\frac{l}{d}\right)^2} \tag{6}$$

with m, n, l being the mode numbers and a, b, d being the corresponding cavity dimensions. For our cavities, $d \ll a, b$ so the modes with non zero l have frequencies too high to be observed in our experiment.

In practice, the cavity has losses. In a transmission spectrum, we expect the resonances to have a certain width: this width is larger for modes which have more losses (or equivalently, a lower quality factor). We thus expect a transmission spectrum composed of some Lorentzian peaks which center frequencies are given by Eq. (6).

These measurements are important to later study the coupling of the FMR to the cavity resonances. Indeed, this coupling only occurs when the cavity and the ferromagnet are close to resonance. Its strength depends on the position of the magnet inside of the cavity: it is stronger if the magnet is positioned on a vibration antinode of a resonance frequency. We must therefore associate each resonance frequency of the spectra to a eigenmode of the cavity.

To measure the spectrum, we use the same setup as depicted in Fig. 1, without the ferromagnet nor the magnetic field produced by the electromagnet. We make the incident frequency f_A vary for fixed incident power $P_A = 6$ dBm. The signal to the local oscillator always has the same power $P_B = 10$ dBm since it must match the desired operating power and a frequency $f_B = f_A - \Delta f$. The RedPitaya acquires around 100 periods of the sinusoidal down-converted signal, sends the buffer to the computer. The standard deviation of the signal estimated by the computer is proportional to the transmission of the system {cavity+mixer}. The spectrum we obtain is shown in Fig. 2:

Let us make a few remarks. Firstly, we find few sharp and distinct resonances: the blue spectrum is noisy. The well-resolved resonances in the insets validate the detection method and the chosen resolution. After much troubleshooting, we have determined that the poor quality of the spectrum seems unlikely to come from a problem in the detection algorithm or an instability of the generated frequency. We suspect the re-soldering of the antennas to play an important role in varying spectra. Secondly, the theoretical expected resonance frequencies do not perfectly match the measured ones. While some theoretical resonances are close to the observed ones, others simply do not have a match. The small misalignment for observed frequencies may emerge from an oversimplification of the cavity geometry (in reality, its corners are rounded) and imperfections in the reflecting surfaces of the cavity. Thirdly, we were bothered by the sluggish transmission of the buffer from the RedPitaya to the computer which slowed down acquisitions.

An observation hard to interpret is that a transmission spectrum taken with a ferromagnetic sample looks extremely sharp. The different resonant frequencies are clearly resolved and the noise decreases significantly. However, some resonances disappear with respect to the previous spectra and other resonance frequencies are shifted

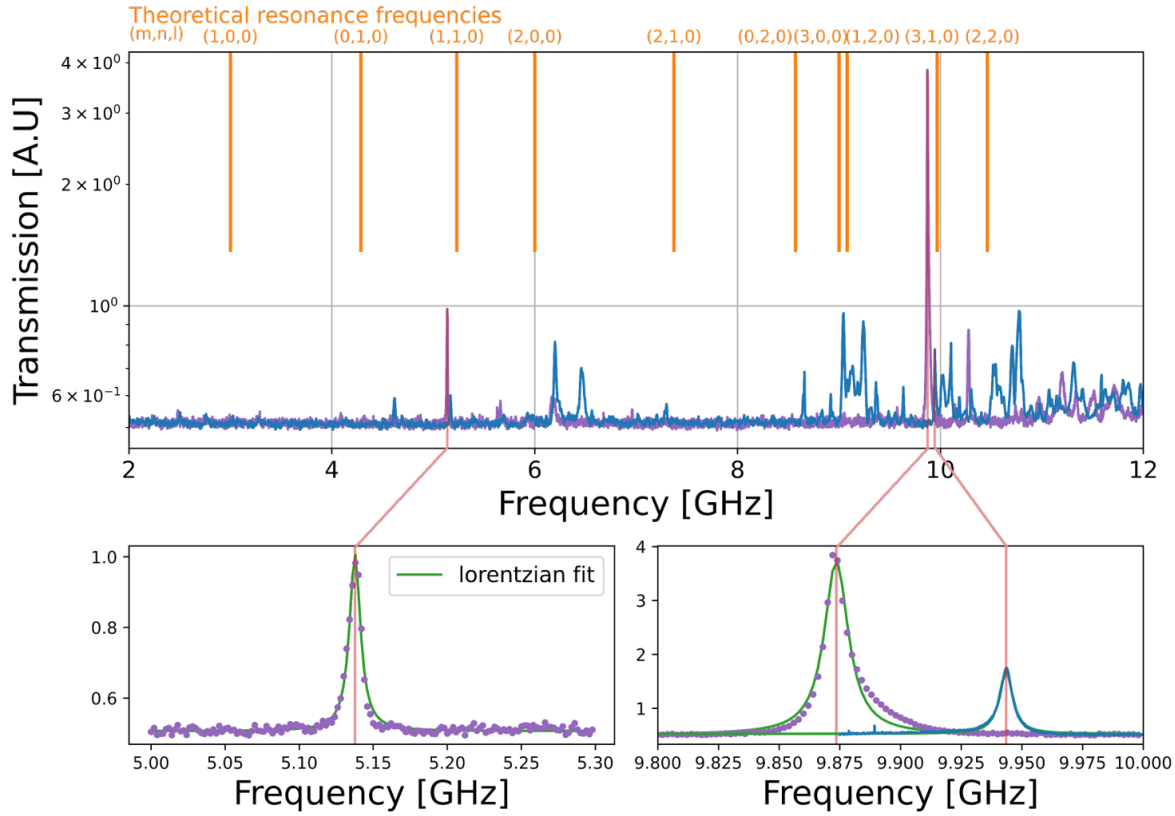

Figure 2: **Large cavity transmission spectra and Lorentzian fit**. The theoretical resonance frequencies of the large cavity (in orange) are in partial accordance with the blue spectrum, but not with the purple spectrum acquired 1 month later, with the medium-sized magnet in the cavity. The frequency on the x-axis corresponds to f_A. The insets focus on the persistent resonances of both spectra. The Lorentzian fit on the blue curve gives the parameters: $f_0 = 9.9435$ GHz and $\Delta f = 3.2$ MHz the full width at half maximum (FWHM)

by values in the range of $50 - 100$ MHz: we imagine that the presence of the magnet has had an influence on the mode structure of the cavity.

2.3 Calibration of the magnetic field

For the FMR to occur, an external uniform magnetic field must be imposed to the ferromagnet. We use an electromagnet to produce such magnetic field, that we calibrate before making any FMR measurements. Indeed, only the current going through the solenoids can be controlled. We relate this quantity to the longitudinal magnetic field $\vec{B} = B\vec{e_z}$, *ie* to obtain the curve $B = f(I_{command})$.

The electromagnet is controlled through ethernet cable with a Delta Elektronika DC Controller. Using the MLX90251 Hall sensor provided, we first manually determine the relationship between the physical current command I_{real} (front potentiometer of the DC generator) and the generated magnetic field. We then relate the computer SCPI command $I_{command}$ to physical current command I_{real}. We proceeded in two steps to make sure we don't go over the 16 A current limit of the electromagnet. The final calibration curve is plotted in Fig. 3.

We observe that the magnetic field is very well described by an affine function up to 800 mT before saturating. The magnetic fields needed in the following, below 600, mT can be obtained in the affine regime. For this calibration, we make sure to keep a separation between the two parts of the electromagnet equal to the width of the cavity, such that the magnetic field intensity is constant for all experiments. We place the Hall sensor at the center and orient it so that the measured signal is the highest, corresponding to the real magnetic field value.

2.4 Characterization of the ferromagnet

Before studying the coupling of the ferromagnet to the cavity modes, we must study the ferromagnet alone to find its resonant frequencies. In order to do so, we place a ferromagnet on the central stripe of a coplanar waveguide (CPW), around the center in the longitudinal direction. The ferromagnet is held in place using tape. We place the

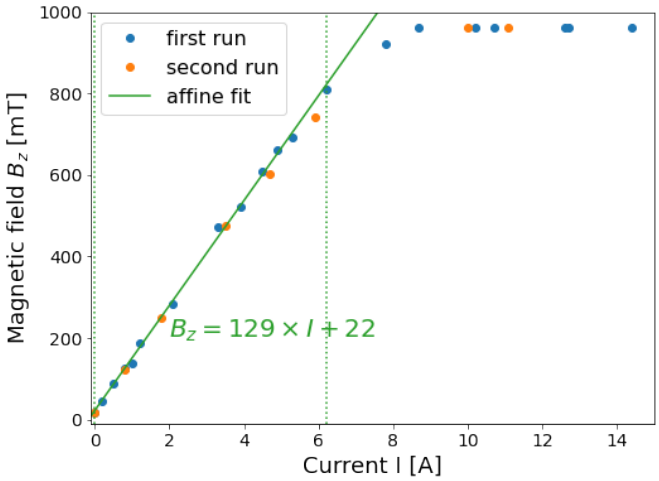

Figure 3: **Magnetic field calibration** The calibration was performed manually in two different runs to verify it could be well reproduced. The generated magnetic field is an affine function up to 800 mT, after which the magnetic field saturates.

waveguide at the center of the electromagnet while making sure that the separation between the two parts of the electromagnet remains equal to the width of the cavity. We connect one end of the waveguide to the microwave source A and the other end is connected to the RF port of the mixer. At a given frequency f_A and magnetic field B, we can thus acquire the transmission of the system.

Since the resonance frequency of the FMR depends on the external magnetic field, we sweep simultaneously the microwave frequency f_A and the external magnetic field B, and measure the transmission of the system. We suspect the electromagnet to take more time than the RF source to stabilize, especially when switching from maximum field intensity to no field. We therefore choose to sweep the frequency over the selected range for each magnetic field intensity, and wait 10 ms for the field to stabilise between each frequency sweep. We acquired transmission spectra for the three YIG samples at our disposal, all differed in size. The results are shown in Fig. 4.

2.5 Coupling of the FMR to the cavity modes

Now that the different components are characterized alone, we bring them together in the setup depicted in Fig. 1. We choose to study the small ferromagnet since the avoided crossing is better observed when the resonances are narrow. In Fig. 4, we can clearly see that the width of the resonances is the smallest with this sample. We glue the ferromagnet to a wall of the cavity. In order to maximize the coupling between the FMR and a cavity mode, we have to place the ferromagnet at the node of the cavity mode. We first identify the observed resonances to the expected modes, estimate at the profile of the considered mode and place the ferromagnet in consequence. However, since the theoretically expected resonances do not match the experimental spectrum, we cannot rigorously apply this method. Instead, we look at the spatial profiles of the lowest frequency modes and find a spot close to a node of several modes in order to maximise our chances of observing an avoided crossing.

To observe avoided crossings, we acquire transmission spectra at the resonant frequencies of the cavity around the corresponding value of B for the FMR. We increase drastically the resolution from Fig. 4.

3 Results

3.1 FMR outside the cavity

In this section, we comment the results of the transmission spectra of the different ferromagnets on the CPW. Several interesting features can be noticed from this figure. First, we see "horizontal stripes" in every spectrum. This can be explained thanks to the first spectrum were there is no ferromagnet on the CPW: the transmission of the microwaves are frequency dependant. This may be due to the transmission frequency response of the CPW or the mixer.

Let's mention that, as expected, we see for each frequency a pronounced decrease in transmission around some value of B: this is indeed the FMR phenomena described previously. The resonance frequency changes as a function of B: by changing B, we modify the Larmor frequency of the ferromagnet.

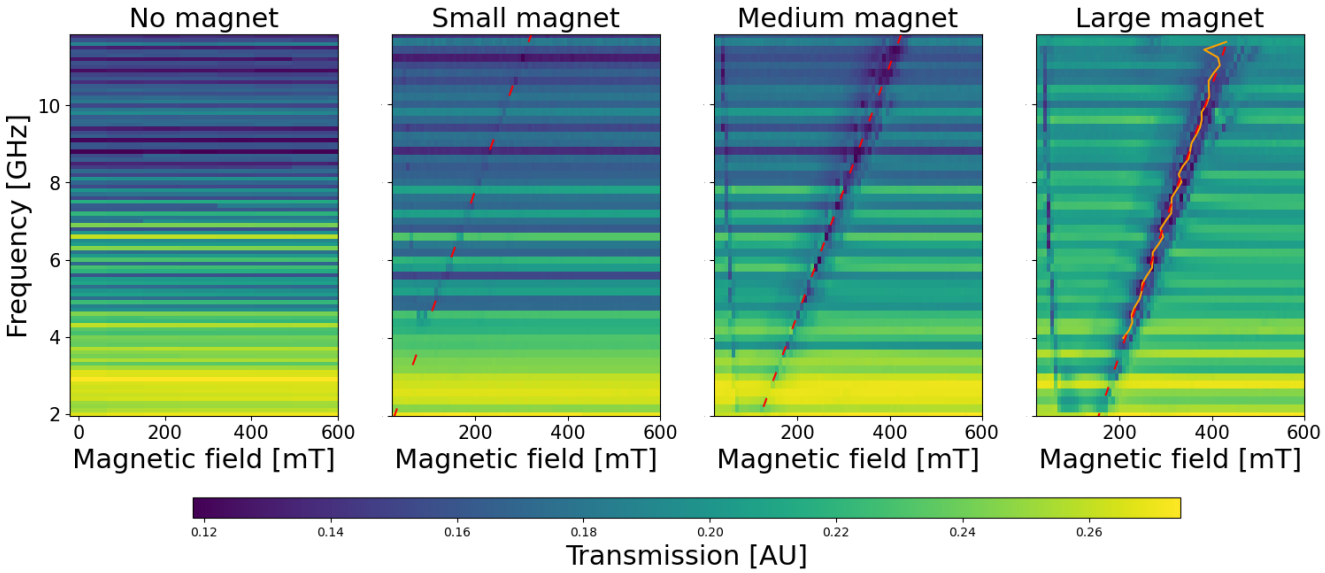

Figure 4: **FMR transmission spectra without coupling to the cavity**. Transmission spectra for ferromagnets of different sizes are plotted. The transmission of the waveguide alone is also plotted to understand the stripes observed. The different acquisitions weren't taken with the same source power nor resolution, so we cannot compare the absolute transmission values between plots. For each spectrum with a magnet, we fit each line with a Lorentzian fit and mark the center of the Lorentzian in orange. These curves are not represent for the small and medium magnet for visibility purposes. We then fit the curve of the centers by an affine fit (red).

Then, the slope of $f_{res}(B)$ depends on the sample. In the theoretical investigations of FMR, an important assumption is than the sample is composed by a single crystal and forms a single magnetic domain, which is certainly not the case for our samples. Furthermore, the relative orientation between the microwave field and the sample orientation plays an important role, but it is a variable we do not control in our experiment. Hence, we cannot apply the general formulas giving $f_{res}(B)$ in our particular case. Furthermore, these formulas do not take into account the size of the samples. We thus find it difficult to understand the differences observed between the different samples. It may result from a difference of orientation of the samples with respect to the magnetic field in the different acquisitions or more subtle effects can play a role. We also observe that the width of the resonances increases with sample size. One hypothesis to explain this could be the following: in a large sample, there are several crystal domains: each one of them will be oriented in a different direction with respect to $\vec{B}$. Therefore, their resonance frequency will be slightly modified, accounting for a broad dispersion in f_{res}. But we also know that this width is related to the damping mechanisms. By studying these mechanisms in more detail and specifically their dependence with size and frequency, we could understand our first observation and also that the frequency width of the resonances increases with the resonant frequency.

We also notice that, at fixed frequency, there are two values for the magnetic field for which we observe an absorption resonance. However, we have no theoretical explanation for the low magnetic field value.

3.2 Coupling to the cavity

When the small ferromagnet is placed inside the cavity, we observe the anti-crossing of the resonant frequencies of the ferromagnet (Fig. 5). According to the large cavity transmission spectrum, there is a resonant frequency at $f_0 = 9.943$ GHz around which transmission sharply increases. We recover this observation in the spectrum below when the external magnetic field is either small or large compared to $B_0 = 275$ mT. When the magnetic field goes through this value, we see that the transmitted frequencies either increase when $B < B_0$ or decrease when $B > B_0$. Indeed, the FMR and the cavity resonances are coupled in this regime, so that the resonant frequencies (corresponding to the eigenfrequencies of the dressed Hamiltonian (Eq. 5) repell each other. When $B < B_0$, the FMR resonant frequency is lower than the cavity mode: when the frequencies repell each other, the frequency corresponding to the transmitted microwave increases. Conversely, when $B > B_0$, the FMR resonant frequency is larger than f_0 so that the dressed cavity mode has a lower frequency. When the two eigenfrequencies are far apart, we recover that the eigenstates of the Hamiltonian can be very well approximated by the uncoupled eigenstates of the FMR and the cavity.

We also perform a numerical simulation of the Hamiltonian in Eq. 5, fine-tuning the parameters to fit the experimental data exhibiting the avoided crossing. The Hamiltonian 5 is solved using Qutip, then the eigenfre-

quencies are artificially broadened using a Lorentzian fit of fixed amplitude and width for any magnetic field or eigenfrequency value. These 'universal' Lorentzian parameters are parameters of the fit, along with ω_c, ω_0, $\tilde{g}$, γ_{eff} and B_{offset}. Fig. 4 assures us that, in the considered magnetic field range, $\omega_c = \gamma_{eff}(B - B_{\text{offset}})$ (slope of the ferromagnetic resonance).

The fit of the numerical simulation outputs a ferromagnetic resonance slope coherent with the estimations from Fig. 4 .

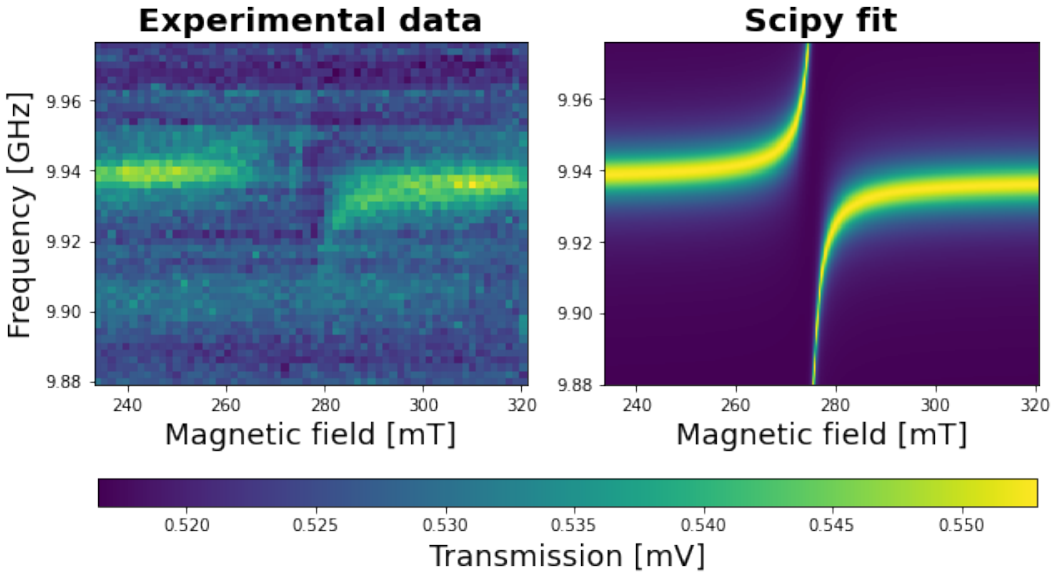

Figure 5: **Coupling of the ferromagnet to the cavity** One recognises an avoided crossing (anticrossing) between both resonance frequencies: the cavity resonance (horizontal line) is perturbed by the ferromagnet resonance (diagonal line, Fig. 4, small ferromagnet). The Hamiltonian (5) was simulated with the python package QuTiP. The Lorentzian fit was implemented with Scipy, with the model parameters: $\tilde{g} = 59.4 \pm 0.1$ MHz, $\gamma_{eff} = 30.5 \pm 0.1$ MHz/mT, $B_{\text{offset}} = 82 \pm 11$ mT. The large uncertainty on B_{offset} is due to the small magnetic field and frequency window, far from the origin. The value for γ_{eff} is coherent with the fit in Fig. 4 for the small ferromagnet ($\gamma_{eff} = 33$MHz/mT).

Conclusion

In this experimental project, we have assembled a setup to observe FMR and its coupling to a microwave cavity's modes. By interfacing the electronics with a computer, we have acquired transmission spectra for varying microwave frequency and external magnetic field. We have observed cavity resonances, FMR in ferromagnetic samples of varying size and finally the expected avoided crossing when both the cavity and FMR are on resonance. Some experimental results are well corroborated by a numerical simulation.

Our experiment could be improved in several ways. First of all, the electronics used in the detection setup were sub-optimal. Even though the RedPitaya STEMLab card offers a straightforward computer connection, the transmission of the buffer to the computer was an order of magnitude slower than the signal measurement itself. This communication speed limited in practice our measurements' resolution due to time constraints. To solve this issue, one could compute the standard deviation of the signal locally on the RedPitaya. Furthermore, the RedPitaya's maximum sampling rate is 150 MHz, very far from the GHz range of the experiment. We had no choice but to use a mixer to perform the down conversion of the signal going through the cavity, even though this electrical components' general influence can hardly be taken into account. Its datasheet does not mention the relation between the power or the phase in the outgoing IF port with respect to the ingoing signals in the RF and LO ports. We believe this may be linked to the horizontal 'stripes' of Fig. 4 , preventing us from measuring absolute transmission instead of the standard deviation of the output voltage. An ideal solution would be to use a computer interfaced network analyser as in [5].

Then, the spectra in Fig. 2 were not always composed of distinct peaks, while some observed peaks did not match the theoretical resonance frequency values. Hence it was impossible to associate a clear spatial profile to a given resonant frequency. As mentioned earlier, this has an influence on the optimal ferromagnet position inside of the cavity. For example, we were unable to distinctly observe the avoided crossing for the low resonant frequencies between 4 and 6 GHz.

Finally, while crystalline orientation plays an important role in such experiments [5], we did not control that parameter. We were not sure on whether the samples we used were formed of a single crystal or several sectors with different orientations. Even though our setup allows to observe certain phenomena associated to FMR, a better designed setup could allow us to unveil more subtleties about this phenomenon and extract more information about our ferromagnetic samples.

References

[1] J. E. Griffiths. "Anomalous High-frequency Resistance of Ferromagnetic Metals". In: *Nature* 158 (1946), pp. 670, 671. DOI: https://doi.org/10.1038/158670a0.

[2] Charles Kittel. "Interpretation of Anomalous Larmor Frequencies in Ferromagnetic Resonance Experiment". In: *Phys. Rev.* 71 (4 Feb. 1947), pp. 270–271. DOI: 10.1103/PhysRev.71.270.2. URL: https://link.aps.org/doi/10.1103/PhysRev.71.270.2.

[3] Charles Kittel. "On the Theory of Ferromagnetic Resonance Absorption". In: *Phys. Rev.* 73 (2 Jan. 1948), pp. 155–161. DOI: 10.1103/PhysRev.73.155. URL: https://link.aps.org/doi/10.1103/PhysRev.73.155.

[4] Orhan Yalçın. "Ferromagnetic Resonance". In: *Ferromagnetic Resonance*. Ed. by Orhan Yalcin. Rijeka: IntechOpen, 2013. Chap. 1. DOI: 10.5772/56134. URL: https://doi.org/10.5772/56134.

[5] Dengke Zhang et al. "Cavity quantum electrodynamics with ferromagnetic magnons in a small yttrium-iron-garnet sphere". In: *npj Quantum Inf* 1 (2015), p. 15014.